ARTICLE - Non-Hodgkin Lymphoma

The IL32/BAFF axis supports prosurvival dialogs in the lymphoma ecosystem and is disrupted by NIK inhibition

Salomé Decombis,[1,2,3] Antonin Papin,[1,2,3] Céline Bellanger,[1,2,3] Clara Sortais,[1,2,3,4] Christelle Dousset,[1,2,3,4] Yannick Le Bris,[1,2,3,5] Thiphanie Riveron,[1,2,3] Stéphanie Blandin,[6] Philippe Hulin,[6] Benoit Tessoulin,[1,2,3,4] Mathieu Rouel,[1,2,3] Steven Le Gouill,[1,2,3,4] Agnès Moreau-Aubry,[1,2,3] Catherine Pellat-Deceunynck[1,2,3] and David Chiron[1,2,3]

[1]Nantes Université, INSERM, CNRS, Université d'Angers, CRCI2NA; [2]L'Héma-NexT, i-Site NexT; [3]GDR3697 Micronit, CNRS; [4]Service d'Hématologie Clinique, Unité d'Investigation Clinique, CHU; [5]Service d'Hématologie Biologique, CHU and [6]SFR-Santé, INSERM UMS016, CNRS UMS 3556, FED 4202, Nantes Université, CHU, Nantes, France

Correspondence: D. Chiron
david.chiron@univ-nantes.fr

Received: August 11, 2021.
Accepted: February 9, 2022.
Prepublished: March 10, 2022.

https://doi.org/10.3324/haematol.2021.279800

Supplemental Files

The IL32/BAFF axis supports prosurvival dialogs in the lymphoma ecosystem and is disrupted by NIK inhibition

Decombis et al.

Supplemental information includes supplemental Methods, 3 supplemental tables, 9 supplemental figures and legends and supplemental references

Supplemental Methods

MCL cell lines

JeKo-1, MINO, REC-1, MAVER-1, and GRANTA-519 were purchased from DSMZ (Braunschweig, Germany) and Z138 from ATCC (Manassas, USA). UPN1, HBL2 and SP53 were kindly provided by Prof. V. Ribrag (Institut Gustave Roussy Villejuif, France), Prof. M Callanan (INSERM, CHU de Dijon, France) and Prof. S. Chen-Kiang (Cornell University, NY), respectively. NTS3 cell line has been generated in our laboratory (characterized by GEP, GSE86322). Cell lines are routinely identified using a flow cytometry-based barcode as well as MHC class I sequencing[1].

Genome editing using the CRISPR-Cas9 system

To generate IL32$^{-/-}$ MCL cells, we infected MINO and NTS3 cells with lentiviruses encoding for Cas9-mcherry (Addgene plasmid # 70182), and mCherry positive cells were sorted using FACSAria Cell sorter (Cytocell, SFR Bonamy, Nantes). Sorted cells were then infected with lentiviruses containing *GFP* and doxycycline-inducible sgRNA (Addgene plasmid # 70183) directed against IL32. The designed crRNA targeted the following sequence in *IL32* gene: 5'-GGCCGCCATGTGCTTCCCGA-3'. GFP positive cells were sorted and sgRNA expression was induced. Cells were cloned by limiting dilutions from the bulk prior characterization of IL32 knockout by DNA sequencing and protein analysis (Figure S7).

Secretome quantification

Monocytes were differentiated with CSF1 (50 ng/mL) with or without (rh)IL32β (100 ng/ml) during 3 days, supernatant was collected and soluble factors were quantified by cytokine array (Proteome Profiler Human Cytokine Array Kit, R&D Systems). Pixel densities were analyzed by using the Image Lab Software (Bio-Rad). Regarding IL32, concentration was determined in MCL cell line supernatants using Human IL32 duoset Elisa (R&D systems). BAFF concentration was determined using Human BAFF / TNFSF13B Elisa kit PicoKine^{TM} (Boster).

Bioinformatics analysis

Gene Expression Profiling (GEP)

.CEL files were downloaded and processed in R-3.6.1 using the affy package, optical noise/background correction was performed by gcrma with standard options, and expression batches were finally normalized by quantiles using the limma package. Differential gene expression was assessed with limma package (up regulated gene: log2Fc>0.5; adjusted

p<0.05) and we used the GAGE package (KEGG pathway analysis) for gene set enrichment analysis.

Full-length RNA-seq:

Total RNA was extracted with RNeasy Mini kit (Qiagen) and quantified using a Nanodrop®ND-1000 spectrophotometer (Thermo Scientific). Quality and integrity of RNA samples were assessed using the 2100 Bioanalyzer and RNA 6000 Nano LabChip kit series II (Agilent Technologies). Library construction was performed from 500ng of total RNA with SureSelect Strand-Specific RNA Library Prep for Illumina Multiplexed kit (Ref 5190-6410, Agilent Technologies) according to Agilent_PrepLib_G9691-90010_juillet2015_vD protocol. Purifications were carried out with NucleoMag NGS Clean-up and Size Select (Ref 744970.50, Macherey-Nagel). Fragments size of libraries was controlled on D1000 ScreenTape with 2200 TapeStation system (Agilent Technologies). Libraries with P5-P7 adaptors were specifically quantified on LightCylcer ® 480 Instrument II (Roche Life Science) and normalized with DNA Standards (1-6) (Ref KK4903, KAPABIOSYSTEMS - CliniSciences). Each library was pooled and prepared according to Denaturing and diluting libraries protocol for the Hiseq and GAIIx, part#15050107 v02 (Illumina) for cluster generation on cBotTM system. Paired-end sequencing (2x100 cycles) was carried out with 4 samples by lane on HiSeq® 2500 system (Illumina) in TruSeq v3 chemistry according to the instructions of HiSeq® 2500 System Guide, part#15035786 v01 (Illumina).

After demultiplexing and quality control with fastQC_0.11.2 (http://www.bioinformatics.babraham.ac.uk/projects/fastqc/), illumina adapter were trimmed with cutadapt-1.2.1[2] and reads with Phred quality score below 30 were filtered with prinseq-lite-0.20.3[3]. Reads were aligned against human hg19 reference genome with tophat2.0.10[4], reads count and differential analysis was realized with Gfold[5].

Relative abundance of 9 known transcripts of IL32 was performed with Pennseq[6] using refseq annotation downloaded from UCSC.

3'seq-RNA Profiling

3'seq-RNA Profiling protocol is performed according to Soumillon et al.[7] The mRNA poly(A) tails are tagged with universal adapters, well-specific barcodes and unique molecular identifiers (UMIs) during template-switching reverse transcriptase. Barcoded cDNAs from multiple samples are then pooled, amplified and tagmented using a transposon-fragmentation approach, which enriches for 3′ends of cDNA. A library of 350–800 bp length is run on an Illumina NovaSeq 6000 using NovaSeq 6000 SP Reagent Kit 100 cycles (ref #20027464).

Raw fastq pairs used for analysis matched the following criteria: the 16 bases of the first read correspond to 6 bases for a designed well-specific barcode and 10 bases for a unique molecular identifier (UMI). The second read (58 bases) corresponds to the captured poly(A) RNAs sequence. We perform demultiplexing of these fastq pairs according to the samplesheet to generate one single-end fastq for all samples. These fastq files are then aligned with bwa to the reference mRNA sequences and the mitochondrial genomic sequence, both available from the UCSC download site. DGE profiles are generated by parsing the alignment files (.bam) and counting for each sample the number of unique UMIs associated with each RefSeq genes. Reads aligned on multiple genes, containing more than one mismatch with the reference sequence or reads containing a polyA pattern are discarded. Finally, a matrix containing the expression of all genes on all samples is produced. The expression values, corresponding to the absolute abundance of mRNAs in all samples, is then ready for further gene expression analysis. DESeq2 is used to normalize expression with the DESeq[8]. Normalized counts are transformed with vst (variance stabilized transformation) function from DESeq library. Batch effects may be corrected with the limma library function "removeBatchEffect".

***IL32* locus-specific methylation analysis**

Genomic DNA was extracted with QIAamp DNA Blood Mini kit (Qiagen) and treated with bisulfite (Active-Motif). The converted DNA was amplified by specific nested PCR for promoter and CpG island of *IL32* (Table S3). The cloning step was realized with StrataClone PCR Cloning Kit (Stratagene). Extracted DNA from the selected colonies (Miniprep Plasmid DNA purification, Macherey Nagel) was sequenced and analyzed (n=8 clones per sample).

Immunohistochemistry (IHC)

Classic IHC

Formalin-fixed paraffin-embedded (FFPE) tissue sections of 3 lymph nodes and 1 spleen from 4 MCL patients were obtained from Pathological Anatomy Department, CHU, Nantes, France. For IHC staining, the sections were subjected to pretreatment involving antigen retrieval by heating in EDTA buffer. Samples were then incubated with an anti-IL32 antibody and with the Impath DAB OB Sens Detection kit (A. Menarini Diagnostics, France) for revelation. The experiment was realized in the automated Impath36 (A. Menarini Diagnostics, France). Histopathology slides were scanned with a Nanozoomer 2.0 HT (Hamamatsu Photonics K. K., Japan). Negative controls for IHC were included in each run, and consisted in replacing the primary antibody with Rabbit Primary Antibody Isotype Control (2 µg/mL IgG) (GBI Labs, USA).

Other methods

Viability assays (Annexin-V staining) as well as real-time quantitative reverse transcription polymerase chain reaction (RT-qPCR, control gene RPL37A) and immunoblot protocols have been previously described [9]. Statistical analyses were performed using two-sided Mann–Whitney, Wilcoxon-matched pairs signed-rank, or t-tests as stated in the Figure legends. Analyses were performed using Graph-Pad Prism and R statistical softwares and all tests were considered statistically significant at $p < 0.05$.

Supplemental Tables

MCL#	Age	Status	%CD19+/CD5+	Subtype at D	SOX11	TP53	Constitutive IL32
1	74	D	57	LNN	-	wt	-
2	22	R	75	Conventional	+	wt	-
2_PE	69	R	75	Conventional	+	wt	+
3	73	D	80	Conventional	+	wt	-
4	66	D	80	Conventional	+	wt	+
5	73	R	67	Blastoid	+	abn	+
6	65	D	43	LNN	-	wt	-
7	80	R	77	Conventional	+	wt	-
8	81	R	66	LNN	-	abn	-
9	73	R	70	Conventional	*ND*	wt	*ND*
10	60	D	87	LNN	-	wt	-
11	74	D	87	Conventional	+	wt	-
12	82	D	92	Conventional	+	wt	-
13	78	R	94	LNN	-	wt	-
14	81	R	22	Conventional	+	wt	+
15	75	D	88	Blastoid	+	abn	-
16	71	R	90	Blastoid	+	wt	-
17	80	R	78	Conventional	+	wt	+
18	70	R	79	Conventional	*ND*	abn	*ND*
19	60	R	77	Conventional	+	wt	-
20	60	D	50	Conventional	*ND*	wt	*ND*
21	68	D	60	LNN	-	abn	-
22	57	D	68	Conventional	+	wt	-
23	53	D	35	LNN	-	*ND*	-

Lines	SOX11	TP53	Constitutive IL32
HBL2	+	abn	-
Jeko	+	abn	+
GRANTA	+	wt	+
Z138	+	wt	-
UPN1	+	abn	-
REC1	+	abn	-
MINO	+	abn	+
SP53	+	wt	-
NTS3	+	wt	-
MAVER	+	abn	-

Supplemental Table S1

Patient samples and cell lines information. D, Diagnosis; R, Relapse; LNN, Leukemic Non Nodal. wt: wild type, abn: abnormal.

All samples came from peripheral blood excepted 2_PE form Pleural Effusion

SOX11 and IL32 expression were determined by 3'seq-RNA Profiling of peripheral blood samples. TP53 status was determined by targeted sequencing of *TP53* and/or in vitro response to Nulin3a.

Primary antibodies for Immunoblot			
Specificity	**Clone**	**Source**	**Reference**
Anti Actin	C4	Merck Millipore	MAB1501
Anti GAPDH	G-9	Santa Cruz	sc-365062
Anti IL-32	Polyclonal	Atlas Antibodies	HPA029397
Anti NF-KB p52-p100	Monoclonal	Merck	05-361
Anti NF-KB Anti p50-p105	Polyclonal	Santa cruz	sc-114
Anti Stat 3 (P) Tyr-705	D3A7	Cell signaling	9145
Anti Stat 3	Monoclonal	Biosciences	610190
Anti IκBα (P) Ser 32/34	5A5	Cell signaling	9246S
Anti IκBα	Polyclonal	Cell signaling	9242S
Anti MCL1	22	Santa Cruz	sc-12756
Anti A1	D1A1C	Cell signaling	#14093S
Anti BclxL	D3	Santa Cruz	sc271121

Antibodies and reagents for flow-cytometry		**Clone**	**Source**
Phenotype	anti-CD14-PE	RMO52	Beckman coulter
	anti-CD163-APC	REA812	BD Pharmingen
	Anti-BAFFR-PE	8A7	eBiosciences,
	Anti-BAFFR-PE	11C1	BD Pharmingen
Viability	Annexin V-APC		Beckman coulter

Antibodies and reagents for IHC		**Clone**	**Source**
Antibodies	IL32	Polyclonal	Atlas Antibodies
	Cyclin D1	SP4	Thermo Scientific
	CD3	Polyclonal	Dako
	CD68	PG-M1	Dako
Retrieval solutions	Envision FLEX Target Retrieval solution High pH		Dako
	TR1 Retrieval solution		A. Menarini Diagnostics

TaqMan gene expression assays		**Source**
IL1a	Hs00174092_m1	Applied Biosystems
IL1b	Hs01555410_m1	
IL6	Hs00174131_m1	
IL24	Hs01114274_m1	
IL32	Hs00992441_m1	
BAFF	Hs04234384_m1	
CXCL8	Hs00174103_m1	
RPL37A	Hs01102345_m1	

Reagents and antibodies for treatment		**Source**
Drugs	NIK SMI1	MedChemExpress
	Ibrutinib, BMS-345541	SelleckChem
Neutralizing antibodies	Anti-BAFFR, Anti-BAFF	R&D Systems
Cytokines	IL1a, IL1b, IL10, IFNg, April, BAFF, CSF1, CSF2	Peprotech
	IL6, IL18, IL24, IL32b, TNFa,Wnt5a	R&D Systems
	IGF1	Sigma-Aldrich
	IL15	Serotec

Supplemental Table S2: Antibodies and reagents

Specific nested PCR for CpG island (CPGI): PCR1 F1-R1 and PCR2 F2-R2	
Primer name	Sequence
IL32CPGI-F1	GAGGATTTTTTGGGGAGGAGGGTGT
IL32CPGI-R1	AACACCAAAACCCACACAAACCTTA
IL32CPGI-F2	TGAGATATTTTTTTTTTTTTATATT
IL32CPGI-R2	TACTCTTAAACCCACCCAACTAAAC
Specific nested PCR for promoter: PCR1 F3-R3 and PCR2 F2-R3	
Primer name	Sequence
IL32promoter-F3	AGGTTTAGTTAGGTTGGAGGGTTAG
IL32promoter-R3	CAAACAAAAACAAAAACAAAAACAA
IL32promoter-F2	GGGGAGTTTTAAGATTGTTGAGATT

Supplemental Table S3

IL-32 promoter and CpG island nested PCR primers for methylation analysis

A

Gene_Name	Regulation	log2FC	Top Prediction	score (%)	source
IGFBP3	Up in LN	7.55	Extracellular region	91	PSORT
IL32	Up in LN	6.53	Extracellular region	44	PSORT
COL6A3	Up in LN	6.44	Extracellular region	50	PSORT
PTGDS	Up in LN	6.43	Extracellular region	78	PSORT
RARRES2	Up in LN	6.43	Extracellular region	97	PSORT
FN1	Up in LN	6.42	Extracellular region	53	PSORT
APOC1	Up in LN	6.42	Extracellular region	100	PSORT
CCL21	Up in LN	6.41	Extracellular region	100	Yloc
CXCL9	Up in LN	6.36	Extracellular region	100	Yloc
CLU	Up in LN	6.24	Plasma membrane	47	PSORT
C1S	Up in LN	6.07	Extracellular region	75	PSORT
PRRX1	Up in LN	5.80	Nucleus	100	PSORT
PLA2G2D	Up in LN	5.77	Extracellular region	97	PSORT
MMP9	Up in LN	5.59	Extracellular region	59	PSORT
APOE	Up in LN	5.55	Extracellular region	78	PSORT
VWF	Up in LN	5.54	Extracellular region	81	PSORT
C3	Up in LN	5.53	Extracellular region	91	Yloc
CPE	Up in LN	5.16	Extracellular region	99	Yloc
ADAMDEC1	Up in LN	5.13	Extracellular region	78	PSORT
C10orf10	Up in LN	5.06	Mitochondrion	47	PSORT
LTF	Up in LN	5.03	Extracellular region	75	PSORT
C1QA	Up in LN	5.03	Extracellular region	63	PSORT

B

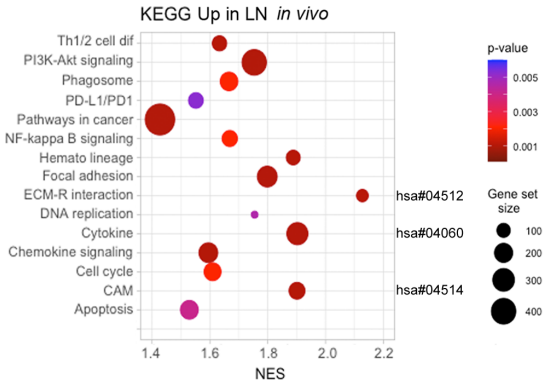

C

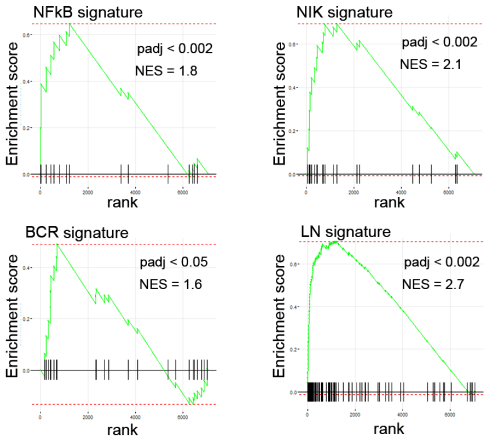

D

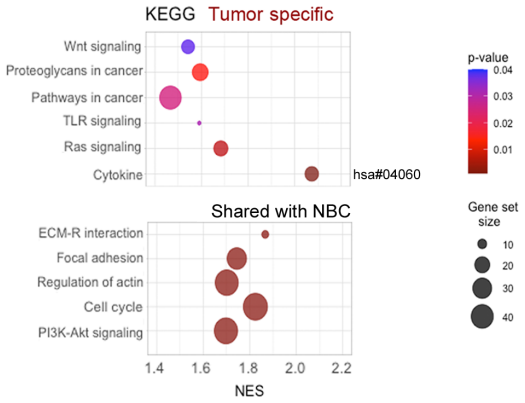

Supp. Fig. S1_Functional annotations and signature enrichment in vivo and ex vivo

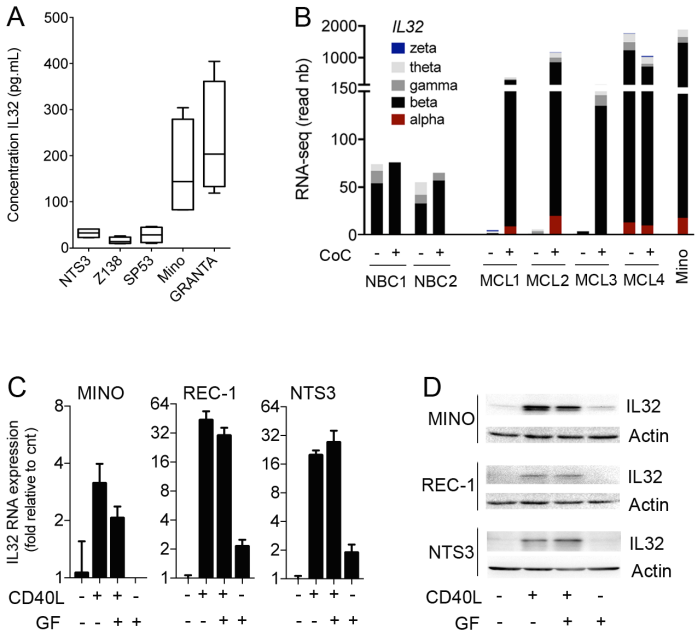

Supp. Fig. S2 _ IL32 is expressed and induced by CD40L in MCL cell lines

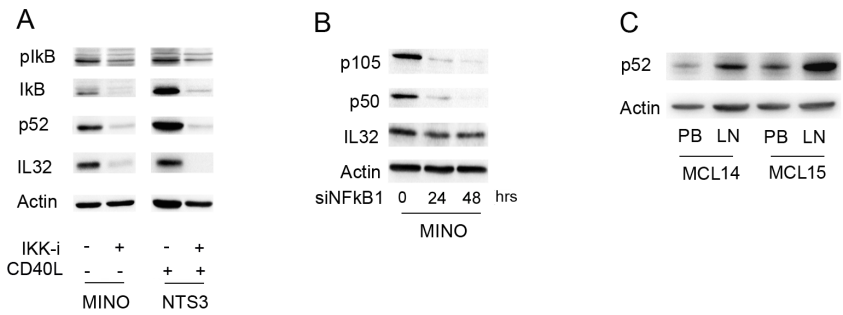

Supp. Fig. S3_ Alternative but not classical NFkB is involved in CD40-induced IL32 expression

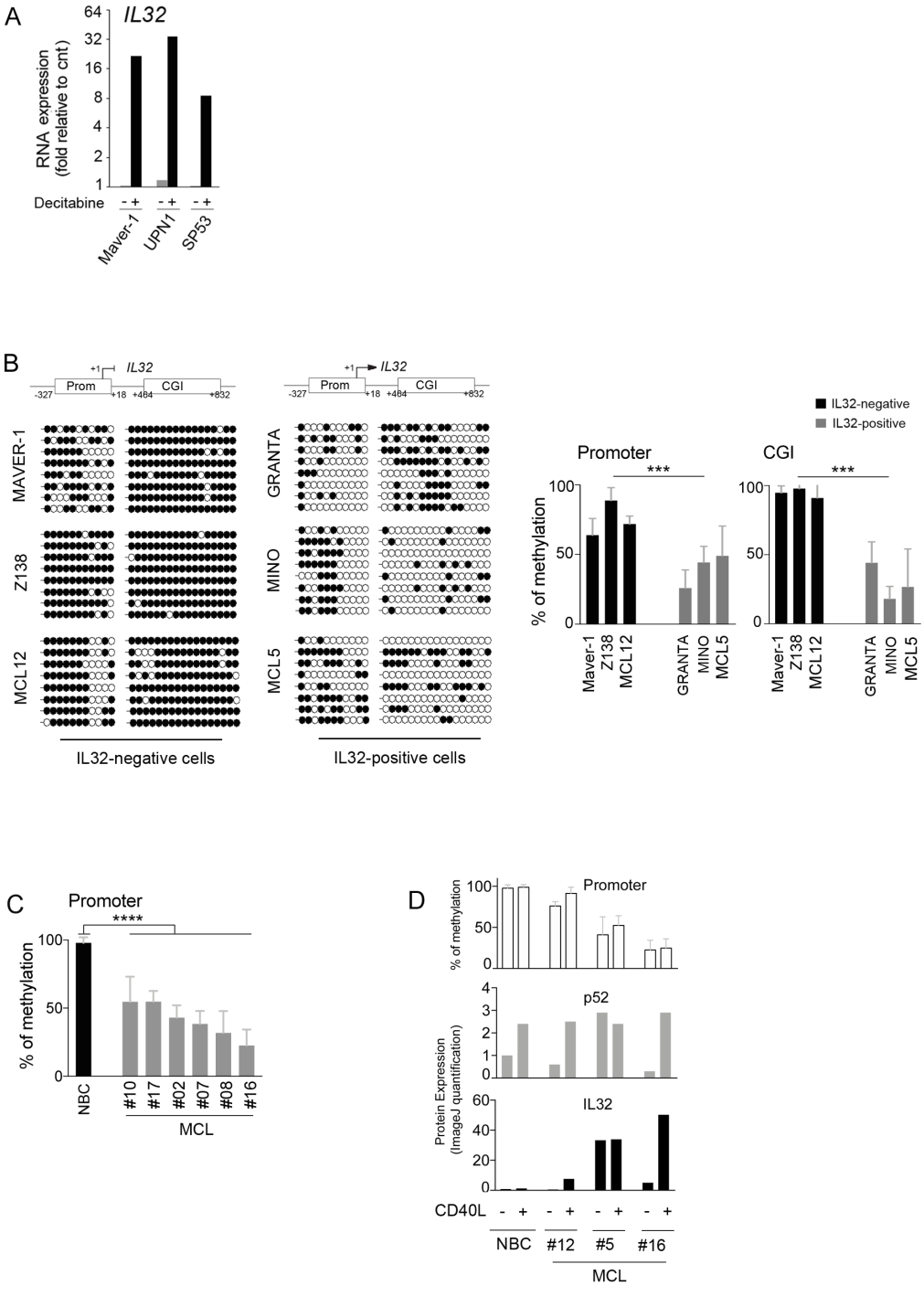

Supp. Fig. S4_Tumor-specific expression of IL32 is due to epigenetic regulations

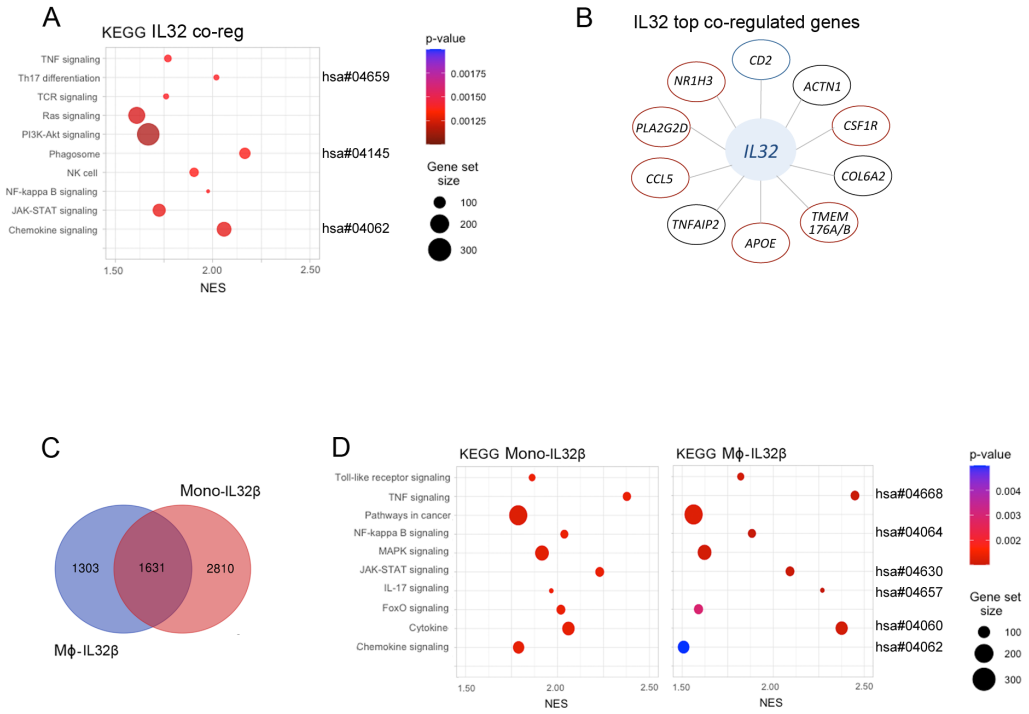

Supp. Fig. S5_IL32 is coregulated with genes expressed by monocytes and T cells in MCL LN

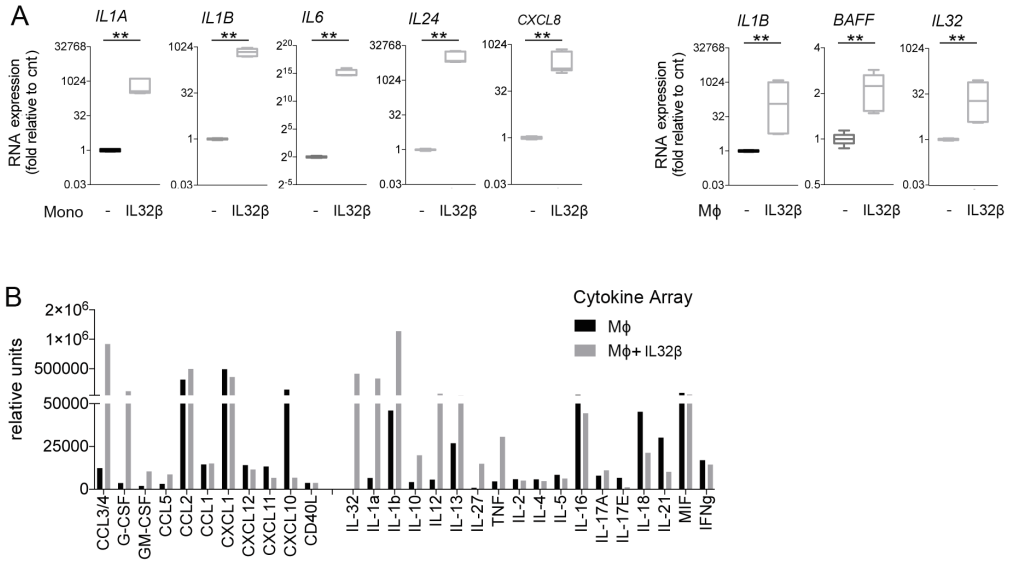

Supp. Fig. S6_ Secretome of IL32-stimulated monocytes and macrophages

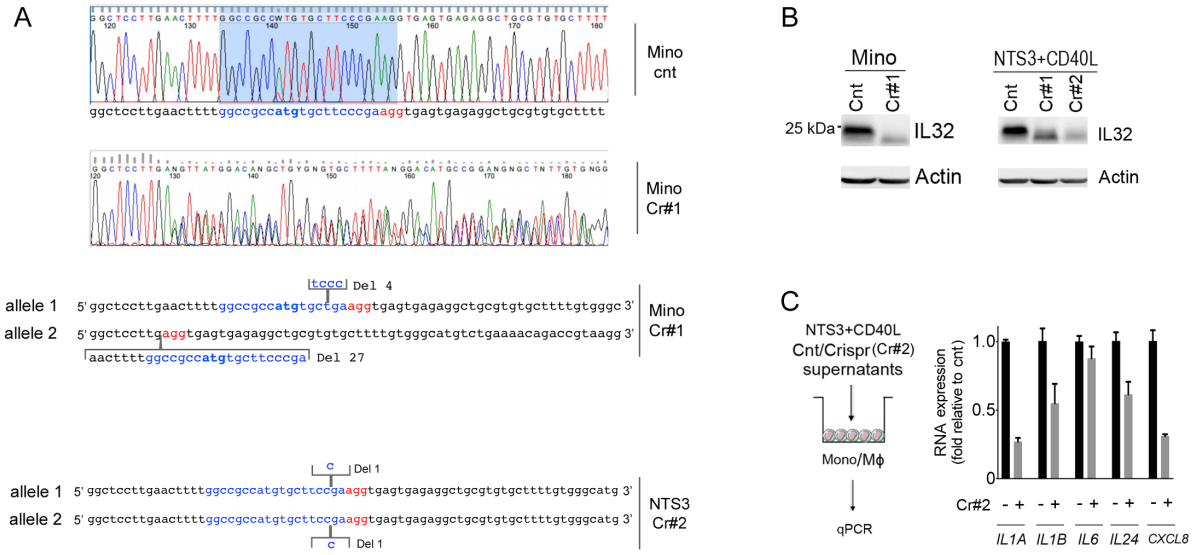

Supp. Fig. S7_ Generation of IL32KO Mino and NTS3 cells through Crisp/Cas9 technology

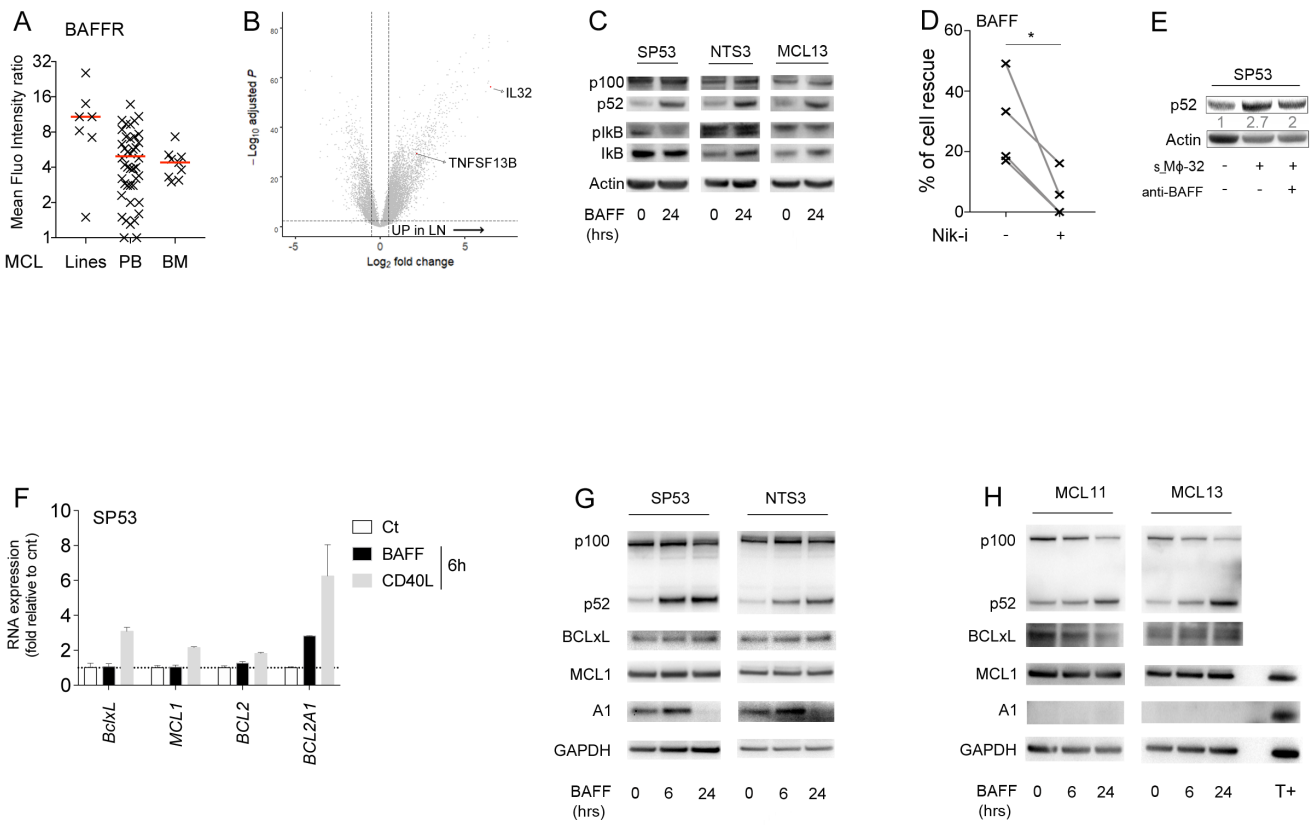

Supp. Fig. S8_ BAFF-specific MCL cell rescue is dependent on alternative NFkB pathway

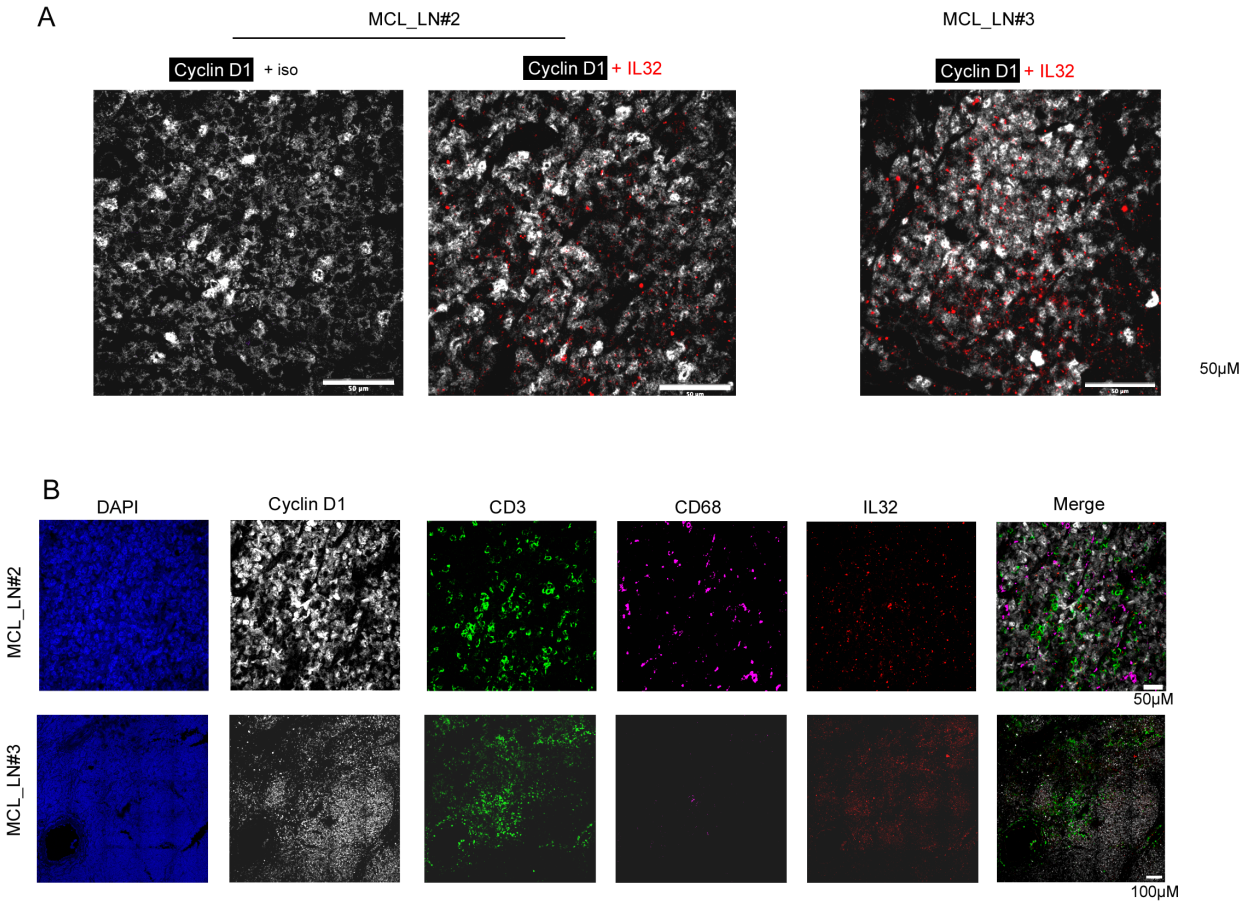

Supp. Fig. S9_ Individual stainings and controls of the multiplex immunohistochemestry experiment

Supplemental Figure Legends

Figure S1. Functional annotations and signature enrichment *in vivo* and *ex vivo*. (**A**) Top significantly modulated genes in LN compared with PB (GEP, log2Fc > 5; n= 22) and their localization by using the Compartments resources[10]. **(B)** KEGG pathway enrichment analysis of the *in vivo* LN upregulated gene set as represented in Figure 1B (n=4584 genes). The x-axis represents the normalized enrichment score (NES) as described by Joly et al. [11]. **(C)** Enrichment plots of the NFkB, NIK and BCR signatures (as described by Saba and colleagues[12]) or LN signature (100 most strongly upregulated genes in LN compared to PB MCL *in vivo*) analyzed using GSEA and reflecting the relevance of our *ex vivo* culture model previously described[9]. **(D)** KEGG pathway enrichment analysis of the "Tumor-specific" (n=1269 genes) and the "Shared with NBC" (n=1948 genes) gene sets as define in Figure 1B. The x-axis represents the normalized enrichment score (NES).

Figure S2. IL32 is expressed and induced by CD40L in MCL cell lines. (A) Concentration of IL32 protein determined by ELISA in the supernatant of NTS3, Z138, SP53, MINO and GRANTA cells. **(B)** *IL32* isoforms prediction by RNA-seq in Mino cells or primary NBC (n=2) and MCL cells (n=4) cultured or not on CD40L expressing cells for 7 days. **(C-D)** IL32 expression in MINO, NTS3 and REC-1 cells cultured on CD40L-expressing cells with or without growth factors (IL10, BAFF, IGF1, IL6) during 24h measured using RT-qPCR **(C)** or immunoblot **(D)**.

Figure S3. Alternative but not classical NFkB is involved in CD40L-induced IL32 expression. (A) Immunoblotting of indicated proteins in MCL cell lines in the presence or absence of the IKK inhibitor BMS-345541 (IKK-i, 5 µM, 6h) in Mino cells or NTS3 cells cultured on CD40L expressing cells. **(B)** Immunoblotting of indicated proteins in MINO cells treated with siRNA against *NFKB1* for 24 to 48h. **(C)** p52 protein expression in primary MCL cells (MCL14 and MCL15) from PB or LN was assessed.

Figure S4. Tumor-specific expression of IL32 is due to epigenetic regulations. (A) RT-qPCR analysis of *IL32* gene expression in Maver-1, UPN1 and SP53 cells treated or not with Decitabine (5'Aza) during 48h. **(B)** Left panel: Detailed locus specific bisulfite sequencing of *IL32* gene (promoter and CpG island) for indicated cells as described in the Methods. Black dots represent methylated CpG island. Mann-Whitney test. *p < 0.0261. Right panel: Locus specific bisulfite sequencing of promoter and CpG islands (CGI) of *IL32* gene for IL32 negative MCL cells (MAVER-1, Z138 and MCL cells (MCL12)) and IL32 positive cells (GRANTA, MINO and MCL cells (MCL5)). For all samples, PCR products were cloned and 8 were sequenced and analyzed as detailed in the Figure S4. Mann-Whitney test. ***p < 0.0002. **(C)** Locus specific bisulfite sequencing of the promoter of *IL32* gene in primary

$CD19^+$ $CD5^+$ NBC (n=1) or MCL (n=6) cells as in panel D. Mann-Whitney test. ****p < 0.0001. **(D)** Integration of the percentage of methylation analyzed by locus specific bisulfite sequencing of the promoter of *IL32* gene and the quantification of p52 and IL32 protein expression (immunoblotting) in NBC and MCL cells at D0 and after culture on CD40L-expressing cells for 7 days.

Figure S5. IL32 is coregulated with genes expressed by monocytes and T cells in MCL LN. (A) KEGG pathway enrichment analysis for the genes co-regulated with *IL32* gene in MCL cells. **(B)** IL32 top co-regulated genes in LN versus PB MCL cells were defined with the limma package. Genes related to macrophages (red circles) or T-cells (blue circles) functions are highlighted. **(C)** Comparison of the induced genes in both macrophages and monocytes treated with (rh)IL32β, as described in Figure 5 **(D)** Common KEGG pathway enrichment found in both macrophages and monocytes treated with (rh)IL32β, as described in Figure 5. The x-axis represents the normalized enrichment score (NES).

Figure S6. Secretome of IL32-stimulated monocytes and macrophages. (A) RT-qPCR analysis of *IL1A, IL1B, IL6, IL24, CXCL8, IL1B, IL32, BAFF* in monocytes or monocytes-derived macrophages cultured with (rh)IL32β for 24h or 48h respectively. Mann-Whitney test. **p < 0.005. **(B)** A pre-defined panel of soluble factors was measured by cytokine array (Proteome Profiler™, Human Cytokine Array, R&D Systems®) in the supernatant of monocytes-derived macrophages stimulated with CSF1 with or without (rh)IL32β for 3 days.

Figure S7. Generation of $IL32^{-/-}$ Mino and NTS3 cells through Crisp/Cas9 technology. (A) DNA sequencing of wild type (Cnt, upper panel) and $IL32^{-/-}$ (Cr#1, lower panel) Mino cells. Deletions are predicted for both alleles. Blue sequence represents the target sequence; red sequence represents the Pam sequence. **(B)** Immunoblotting of IL32 protein in wild type (Cnt) and $IL32^{-/-}$ MINO (Clone Cr#1) and NTS3 (Clones Cr#1 and Cr#2). **(C)** RT-qPCR analysis of *IL1A, IL1B, IL6, IL24, CXCL8, IL32 and BAFF* genes in monocytes cultured during 24h with wild type (-) or $IL32^{-/-}$ (Cr#1) CD40L-stimulated NTS3 supernatant.

Figure S8. BAFF-specific MCL cell rescue is dependent on alternative NFkB pathway. (A) Flow cytometry analysis of BAFFR expression in MCL cell lines (n=7) and in primary MCL cells from peripheral blood (PB, n=42) and bone marrow (BM, n=9). **(B)** Volcano-plot representation of whole transcriptome analysis (publicly available Affimetrix U133, see Methods) from MCL lymph nodes samples (LN, n=107) compared to MCL peripheral blood samples (PB, n=77) shown in figure 1A annotated for TNFSF13B and IL32. **(C)** Immunoblotting of NFkB pathway proteins in SP53, NTS3 and primary MCL cells (MCL13) cultured with BAFF (50 ng/mL) for 24h. **(D)** Percentage of cell rescue dependent on BAFF in

primary MCL (n=4) cultured with or without NIK inhibitor (NIK-i, 10 µM) for 7 days. Paired t test. *p < 0.05. **(E)** p52 protein expression in SP53 cells cultured with Mϕ-32 supernatant (s_Mϕ-32) for 16h with or without anti-BAFF neutralizing antibody (10 µg/mL) assessed by immunoblotting. **(F)** BclxL, MCL1, BCL2 and BCL2A1 gene expression analyzed by RT-qPCR in SP53 cells stimulated with or without BAFF (50 ng/ml) or CD40L during 6h. **(G)** Immunoblotting of alternative NFkB (p100 and p52) pathway and BclxL, MCL1 and A1 protein expression in SP53 and NTS3 cells cultured with or without BAFF (50 ng/ml) during 6 or 24h. **(H)** Immunoblotting of alternative NFkB (p100 and p52) pathway and BclxL, MCL1 and A1 protein expression in MCL11 and MCL13 MCL primary cells cultured with or without BAFF (50 ng/ml) during 6 or 24h and SP53 as a positive control (T+).

Figure S9. Individual stainings and controls on the Multiplex Immunohistochemistry experiment (A) Multiplex Immunohistochemistry on lymph nodes sections from 2 MCL patients (MCL_LN#2/3) for staining of Cyclin D1 (opal 570 ; white), and IL32 (opal 650 ; red) or Cyclin D1 (opal 570 ; white) and Rabbit Primary Antibody Isotype Control (opal 650 ; red). Scale bars, 50 µm. **(B)** Individual staining of Multiplex Immunohistochemistry on lymph nodes sections from 2 MCL patients: MCL_LN#2 (top panel, Scale bars, 50 µm) and MCL_LN#3 (bottom panel, Scale bar, 100 µm) for Cyclin D1 (opal 570 ; white), CD3 (opal 690 ; green), CD68 (opal 520 ; magenta), IL32 (opal 650 ; red). Nucleus is stained with Dapi.

Supplemental References

1. Maiga S, Brosseau C, Descamps G, et al. A simple flow cytometry-based barcode for routine authentication of multiple myeloma and mantle cell lymphoma cell lines. *Cytometry A*. 2015;87(4):285-288.
2. Martin M. Cutadapt removes adapter sequences from high-throughput sequencing reads. *EMBnet journal*. 2011;17(1):10-12.
3. Schmieder R, Edwards R. Quality control and preprocessing of metagenomic datasets. *Bioinformatics*. 2011;27(6):863-864.
4. Kim D, Pertea G, Trapnell C, Pimentel H, Kelley R, Salzberg SL. TopHat2: accurate alignment of transcriptomes in the presence of insertions, deletions and gene fusions. *Genome biology*. 2013;14(4):1-13.
5. Feng J, Meyer CA, Wang Q, Liu JS, Shirley Liu X, Zhang Y. GFOLD: a generalized fold change for ranking differentially expressed genes from RNA-seq data. *Bioinformatics*. 2012;28(21):2782-2788.
6. Hu Y, Liu Y, Mao X, et al. PennSeq: accurate isoform-specific gene expression quantification in RNA-Seq by modeling non-uniform read distribution. *Nucleic acids research*. 2014;42(3):e20-e20.
7. Magali S, Davide C, Stefan S, Alexander O, Tarjei S. Characterization of directed differentiation by high-throughput single-cell RNA-Seq. *BioRxiv*. 2014.
8. Love M, Anders S, Huber W. DESeq2 vignette. *Genome Biol doi*. 2016;110.
9. Chiron D, Bellanger C, Papin A, et al. Rational targeted therapies to overcome microenvironment-dependent expansion of mantle cell lymphoma. *Blood, The Journal of the American Society of Hematology*. 2016;128(24):2808-2818.
10. Binder JX, Pletscher-Frankild S, Tsafou K, et al. COMPARTMENTS: unification and visualization of protein subcellular localization evidence. *Database*. 2014;2014.
11. Joly JH, Lowry WE, Graham NA. Differential Gene Set Enrichment Analysis: A statistical approach to quantify the relative enrichment of two gene sets. *Bioinformatics*. 2020.
12. Saba NS, Liu D, Herman SE, et al. Pathogenic role of B-cell receptor signaling and canonical NF-κB activation in mantle cell lymphoma. *Blood, The Journal of the American Society of Hematology*. 2016;128(1):82-92.